The 12th International Conference of
International Association for Computer Methods and Advances in Geomechanics (IACMAG)
1-6 October, 2008
Goa, India

Experimental and numerical studies of load transfers and arching effect

B. Chevalier, G. Combe, P. Villard
Laboratoire Sols, Solides, Structures – Risques, Grenoble, France

Keywords: granular matter, arching, Distinct Element Method

ABSTRACT: Experimental and numerical tests of the trap-door problem have been carried out, involving several granular materials. Three phases have been observed in the load transfer mechanism, as the trap-door is moved downward. The classical pattern for the description of this type of problem (a vertical plane of failure at each edge of the trap-door) corresponds to the third phase observed. The previous phases correspond to the maximal load transfer and then to the expansion of the granular material from the bottom to the top of the granular layer. Discrete numerical modelling has been processed to investigate the effects of the particles size and of the shear strength parameters on the mechanisms observed. The respective role of peak and residual friction angles has been identified.

1 Introduction

Granular materials present complex global behaviours strongly depending on the initial state and on the type of solicitations, leading to a great variety of applications (Garca-Rojo, 2005). The problem of the trap-door (Terzaghi, 1936) is a solicitation that hides a lot of technological applications and in particular in civil engineering or in mechanics.
Initially studied by Terzaghi (Terzaghi, 1936; Terzaghi, 1943), the trap-door problem consists in the description of mechanisms occurring in a granular material layer when a trap-door located below is moved. In the sense of Terzaghi, two distinct modes can be highlighted according to the direction in which the trap-door is moved. The passive mode corresponds to a trap-door moved upward while the active mode corresponds to a downward trap-door displacement.
The first description of the failure mechanism (Marston, 1913; Terzaghi, 1943) is based on the assumption that the column of granular material above the trap-door slides vertically with the trap-door while the remaining material is fixed. This assumption leads to the analogy with the problem of stresses in silos initially described by Janssen (Janssen, 1895) and recently discussed (Rotter, 1998; Kolb, 1999; Vanel, 1999).
The problem of the trap-door has been commonly studied in a plan strain conditions (Terzaghi, 1943; Ladanyi, 1969; Vardoulakis, 1981; Tanaka, 1993) and the kinematics of the observed phenomena confirm the existence of a vertical sliding column (Ladanyi, 1969; Vardoulakis, 1981) but not for small displacements of the trap-door. This description can be accepted as far as the displacement of the trap-door is sufficient. The first analytical solutions of the trap-door problem are similar to the one developed by Janssen (Janssen, 1895) for the problematic of silos as he introduced a stress ratio $K = \sigma_x / \sigma_z$ of the horizontal stress σ_x to the vertical stress σ_z.
These analytical solutions considered, for the stress ratio K, the Rankine active pressure coefficient (Rankine, 1857). McKelvey (McKelvey, 1994) preferred the use of the Handy (Handy, 1985) coefficient. Contrary to Janssen who deduced a formulation of the vertical stress occurring in the granular layer from the equilibrium of a horizontal slice of the sliding granular mass, Handy considered the equilibrium of a catenary shaped slice instead.
Despite the question of the value of the stress coefficient, a general acceptance exists concerning the mechanism of a column sliding between vertical interfaces. Nevertheless for small displacement of the trap-door, the observed mechanism differs from the classical description and consists in the movements of failure planes. This transitional state has been described by Vardoulakis et al. (Vardoulakis, 1981) as the propagation of an expanding zone of the granular matter from the bottom to the top of the layer converging to a failure body bounded by two vertical planes, located at each edge of the trap-door. This description implies a varying orientation of the failure planes, depending on the amplitude of trap-door displacement. On the contrary, Tanaka and Sakai (Tanaka, 1993) characterized the transitional state by the continuous propagation of two symmetrical shear bands in a particular direction until they reach the layer top.
The displacement of the trap-door is a crucial parameter of the trap-door problem because it determines the amplitude of the load transfers involved.
Experimental and numerical tests have been carried out to reproduce the trap-door problem in the plain strain

case. The load acting on the trap-door has been monitored or computed during its vertical displacement in order to quantify the macro-phenomena. Photographs taken during tests and numerical view of the granular assembly complete the analysis in a kinematics point of view.

2 Experimental results

2.1 Design of apparatus

The physical model consists of a box 1.0x0.4 m in plan (Fig. 1) with a Plexiglas front. Depending on the case studied the height of the test box ranges from 0.15 m to 0.80 m. As shown on Figure 1, a 0.20x0.40 m trapdoor is located in the bottom side of the box. This trapdoor is incrementally moved downward in order to induce load transfers in the granular layer placed above. The vertical residual effort, called F, applied by the granular layer on the trapdoor is measured with a load cell with an accuracy of 1 N. In order to limit frictional effects of walls on the measurements, the residual effort F is measured in the centred half of the trapdoor (Fig. 1). The mean pressure p acting on the trapdoor is deduced from F and from trapdoor dimensions. A dial test indicator gives the trapdoor vertical displacement called δ. δ ranges from 0 to 0.10 m with an accuracy of 1/10 mm. In terms of the kinematics, the behaviour of the granular layer is deduced from the displacement of horizontal coloured strips of the granular matter by the use of digital image analysis software.

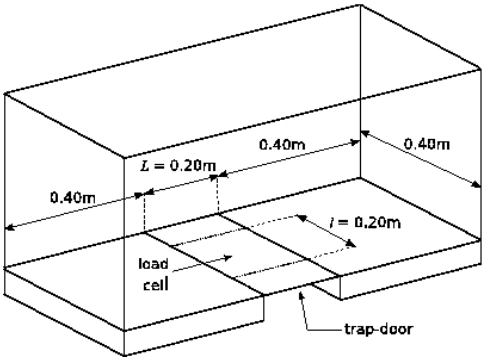

Figure 1. Diagram of the test box

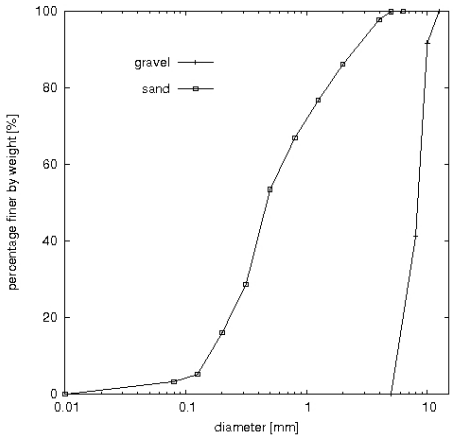

Figure 2. Grading of the materials tested

2.2 Materials

Dry sand and gravel have been tested in a loose initial state. The grading of the granular materials is represented on Fig. 2. The particles shape is almost spherical for the sand and very angular for the gravel. The frictional parameters of the different materials have been deduced from a classical laboratory test: the triaxial test.

Table 1. Physical and mechanical properties of tested materials.

Material	sand	gravel
grain density γ_s [kN/m3]	2610	2650
density in test box γ_i [kN/m3]	1700 ± 50	1517 ± 50
mean diameter D_{50} [mm]	0.5	8.0
φ_p [°]	49.0	56.0
φ_r [°]	42.5	44.5

In order to test the specimens in similar stress states than those observed in the test-box, very low confining stresses have been used: 5 kPa, 10 kPa and 15 kPa. These low confining levels have been obtained by applying an equivalent depression with a vacuum cell.

A peak friction angle φ_p is deduced from the maximal deviatoric stresses reached for each confining pressure with the assumption of a Mohr-Coulomb failure criterion. A residual friction angle has been also measured from the maximal slope of a stable stacking of granular material. φ_r characterizes the minimal shear strength level of the material that should be reached under very large strain level in a triaxial test. Table 1 gives some physical and mechanical characteristics of the different materials tested.

2.3 Procedure

For both sand and gravel, several layer thicknesses h were tested from 0.05 m to 0.60 m. The granular material is poured in the test box with no drop height by 2 cm layers. The granular material obtained is in his loosest state of density. This procedure gives uniform initial apparent density for each material (Tab. 1). Furthermore, for each test, the initial mean pressure acting on the trap is compared to the theoretical value $\gamma_i h$ where γ_i is the initial density of the material. The difference observed between theoretical and experimental values is less than 2 % so that the frictional effect of walls on the measurement of F in the central part of the trap-door can be neglected.

2.4 Mechanisms description

For both granular materials tested, the kinematics involved during trap-door tests break down into three distinct phases. These phases have to be compared to the variation of the pressure p with the trap-door displacement δ (Fig. 3)

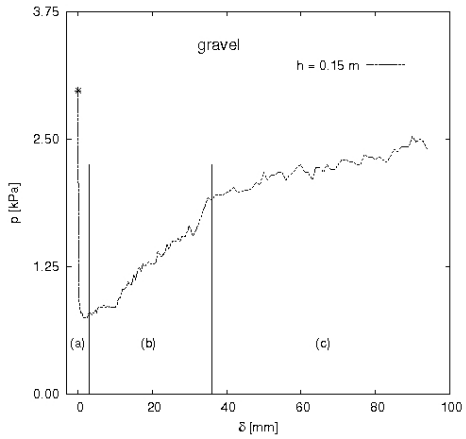

Figure 3. Example of a typical result for a trap-door test p versus δ (gravel, h=0.15 m): (a) first phase, (b) transitional phase, (c) final phase.

The initial mechanism (Fig. 4.a) occurs for very small displacement of the trapdoor (δ≈1-3 mm) and corresponds to the expansion of the granular material located just above the trap-door.

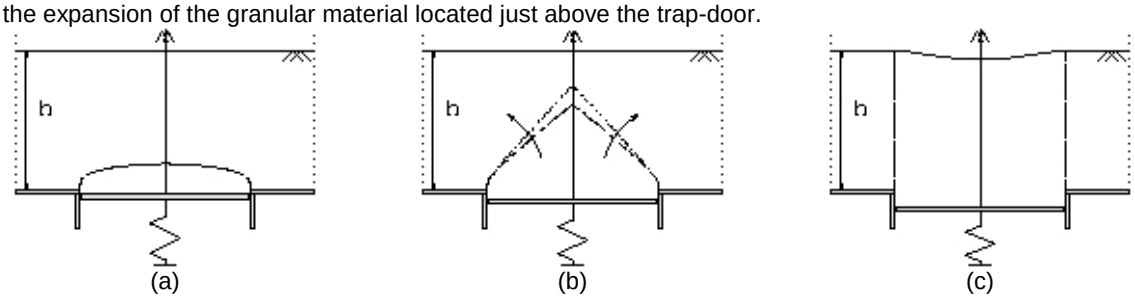

Figure 4. Displacement pattern for the three phases observed during trap-door displacement: (a) first phase, (b) transitional phase, (c) final phase.

The failure boundaries of this area start at each edge of the trap-door in vertical direction and then converge to axis of symmetry of the trap-door. The initial state corresponds to the lowest pressure p_{min} applied on the trap-door (Fig. 3). As shown on Fig. 5, the value of p_{min} is constant as the granular layer thickness exceeds 0.20 m. In addition, the value of p_{min} is lower for the sand than for the gravel.

To this first state succeeds a transitional phase (Fig. 4.b) during which the initial dilatant zone expands until it reaches the surface of the granular layer. This dilatant zone is wedge-shaped until it reaches the surface of granular layer. This phase can be observed for values of δ varying from 1 mm to 40 mm, depending on h and on the material tested. The pressure p increases with a constant rate until it reaches a threshold depending on the granular layer thickness h (Fig. 3). During the transitional phase, the amplitude of load transfers between the subsiding zone and the remaining part of the layer depends on the materials tested. Indeed, no load transfers between subsiding zone and remaining material are observed in the case of the sand, explaining the greater slope of the curve p versus δ during this phase.
The classical failure pattern, called here final state (Fig. 4.c), only occurs after these both first states. The final state corresponds to the vertical alignment of two vertical slipping planes located at each edge of the trap-door. The final state occurs for values of δ increasing with h.

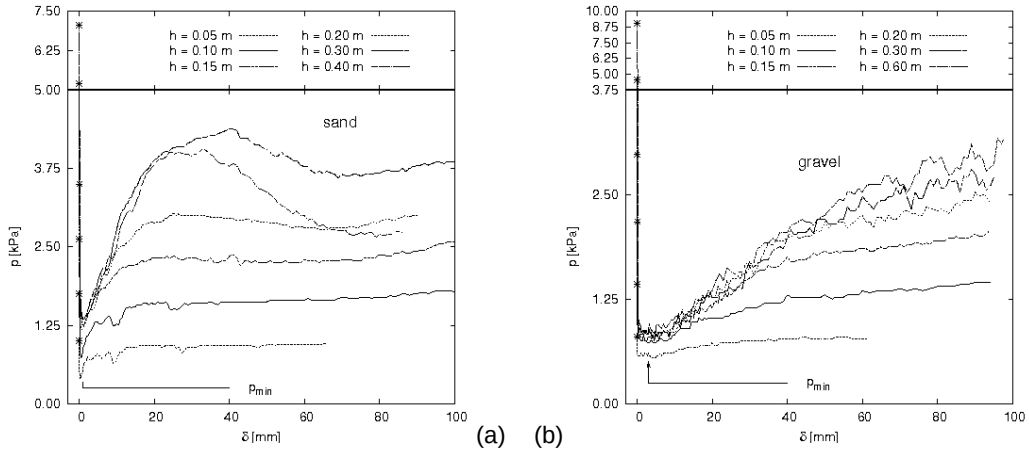

Figure 5. Mean vertical pressure p measured on the trapdoor versus trapdoor downward displacement δ for the sand (a) and for the gravel (b).

2.5 Comparison with analytical solution

Concerning the final phase, the kinematics is analogue for the experimental results and for the solution of Terzaghi (Terzaghi, 1943): two vertical planes of sliding located at each edge of the trap-door (see Fig. 4.c). Experimental and analytical results can be compared. The solution of Terzaghi consists in writing the equilibrium condition in the z-direction of a horizontal slice of thickness dz located between these planes at a vertical axis position z gives the following expression of the stress p_t acting on the trap-door:

$$p_t = \frac{\gamma L}{2K\tan\varphi}\left[1-\exp\left(\frac{-2hK\tan\varphi}{L}\right)\right] \quad (1)$$

with γ the granular material density, L the width of the trapdoor, φ the friction angle of the granular material and K the ratio between horizontal and vertical stresses in the granular material. Terzaghi considered a K ratio defined by $K_a=(1-\sin\varphi)/(1+\sin\varphi)$ which correspond to the Rankine active earth pressure coefficient (Rankine, 1857). The friction angle considered in Eq. 1 and in the expression of K is $\varphi = \varphi_r$, because of the large displacements observed in the granular mass at the final state. However, $K_a\tan\varphi \in [0.158,0.192]$, for $\varphi \in [20°,50°]$ so the influence of the friction parameters of the material on the product $K_a\tan\varphi$ is limited.
The comparison of the pressure p_t obtained with the model of Terzaghi and the experimental results p_f in the final state is shown on Fig. 6.a for the sand and on Fig. 6.b for the gravel.

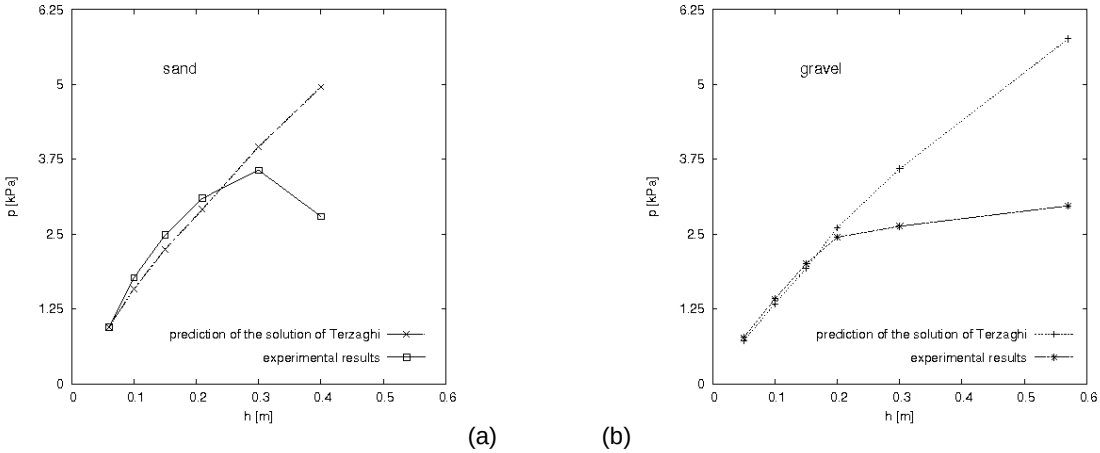

(a) (b)

Figure 6. Comparison of the experimental final value of the pressure measured on the trap-door p_f with the prediction p_t of the model of Terzaghi (Terzaghi, 1943): (a) case of the sand, (b) case of the gravel.

A satisfying correlation exists between experimental results and the predictions of the model of Terzaghi for $h \leq 0.20$ m or in other words, for $h \leq L$. For greater values of h, the prediction given by the solution of Terzaghi overestimates the pressure acting on the trap-door.
Many differences have been observed between both materials with regard to their behaviour in the trap-door test:
- during the first phase with different values of p_{min},
- during the transitional phase with different load transfers amplitude between subsiding zone and remaining part of the granular layer,
- during the final phase with the existence of a peak pressure observed for the sand and not for gravel.
In order to make light of the influence of several parameters such as frictional parameters and particles size, numerical modelling using 3D molecular dynamics has been performed.

3 Numerical results

Distinct Element Method (DEM) is an accurate means to reproduce the behaviour of granular materials such as soils, taking into account both small or large displacements into account. Three materials are tested referred to as C_1, C_2 and C_3. C_1 and C_2 differ only by the size of particles whereas C_2 and C_3 differ by frictional parameters.

3.1 The Distinct Element Method

The modelled granular material is composed on rigid particles that interact with each other through deformable contact points. At each contact point, normal and tangential contact forces are governed by linear contact laws. The normal contact force between two particles i and j can be written $f_n^{ij} = K_n h^{ij}$ where K_n represents the normal stiffness of the contact and h^{ij} the overlap of the two particles i and j. The tangential contact force f_t^{ij} is linked to the tangential incremental relative displacement ε of particles i and j with a stiffness K_t by the expression (Cundall, 1979)

$$\frac{df_t^{ij}}{d\varepsilon} = K_t \qquad \text{with} \qquad \left|f_t^{ij}\right| \leq \mu f_n^{ij} \tag{2}$$

with μ the contact friction coefficient. The integration of Newton's second law – using finite difference – of motion for each particle for a time step allows to calculate the new acceleration for each particle and so to update the positions of the particles of the assembly. The software used here and developed in 3S-R laboratory – SDEC (Magnier, 1997), is based on 3D molecular dynamics principles.

3.2 Assembly generating and testing processes

The numerical assemblies of particles are tested in a test box presenting the same geometry as the experimental device (Fig. 1). The dimensions of the modelled trapdoor are $L=0.20$ m and $l=0.10$ m (for C_2 and C_3). In order to quantify the effect of scale on the load transfers, one test has been carried out with a trap-door

twice wider: $L=0.20$ m and $l=0.20$ m (for C_1). The modelled particles assemblies are set up within this test box without gravity and using the Radius Expansion with Decrease of Friction process (REDF) (Chareyre, 2005). Particle diameters are progressively increased until an isotropic pressure threshold $P_{max}=500$ Pa is reached. The time that this threshold is reached, the porosity η of the assembly (defined by the ratio of the volume of voids to the total volume of the assembly) is assumed to be maximal $\eta = \eta_{max}$. As the isotropic pressure can not be reduced under the threshold, the contact friction coefficient μ is reduced so that the particle expansion can continue. This process is carried on until the contact friction coefficient $\mu=0$. The porosity is then minimal: $\eta=\eta_{min}$. With this process, an assembly can be generated at any porosity included in the range $[\eta_{min}, \eta_{max}]$. After the generation of the assembly, the gravity is applied to the granular material. The trap-door is then moved downward with increment $\delta=1$ mm. The thickness of each granular material layer tested here is equal to $h=0.20$ m.

3.3 Material properties

For each granular assembly, the ratio of the maximal diameter d_{max} of the particles to the minimal one d_{min} is constant equal to $d_{max}/d_{min}=1.25$. In the range $[d_{min},d_{max}]$, each diameter value d is equiprobable. The number of particles is constant for each modelling and equal to 23000. The density of particles is also constant and equal to $\gamma_s=2650$ kg/m^3. The particles, referred to as clusters, is composed of a non divisible assembly of two spheres of same diameter ξ. The distance between both centres is equal to 0.95ξ.

Table 2. Physical and mechanical properties of numerical assemblies.

	Material	C_1	C_2	C_3
Micromechanical properties	d_{min} (mm)	6.58	5.21	5.21
	d_{max} (mm)	17.43	13.87	13.87
	η	0.405	0.405	0.405
	μ	1.466	1.466	0.521
Micromechanical properties	E	5.90	5.90	4.95
	v	0.1245	0.1245	0.1258
	φ_p [°]	46.2	46.2	35.2
	φ_r [°]	31.6	31.6	31.3

The contact stiffness is constant from one assembly to another. The stiffness level κ (Combe, 2003) of the granular assemblies leads to a ratio of the mean contact overlap $<h>$ between two particles to the mean particle diameter $<d>$ to $1/\kappa=(<h>/<d>)=3.10^{-4}$. All assemblies are characterized by a ratio $K_t/K_n=0.75$ between tangential and normal stiffness. Two values of μ have been used (see Tab. 2)
The macro-mechanical characteristics of the granular assemblies are deduced from the modelling of triaxial tests. These tests are modelled with a constant confining stress $\sigma_2= \sigma_3= 5$ kPa and with a constant strain velocity. The shear strength of the granular materials is characterized by two different friction angles. The peak friction angle φ_p represents the highest maximal shear strength of the assembly. The residual shear strength is characterized by the residual friction angle φ_r and occurs for large axial strain rates. Three numerical assemblies have been tested in the trap-door test. The mechanical characteristics of the three assemblies are given in Tab. 2.

3.4 Numerical tests results

The kinematics observed in numerical tests is the same as in experimental tests. The three phases observed experimentally – initial, transient, and final phases – are also observed with the numerical model (Fig. 7 and Fig. 8).
Effect of particle size can be deduced from the comparison of the results with materials C_1 and C_2 (Fig. 8.a). Particles of C_2 are twice smaller in volume as particles of C_1. Effect of the shear strength parameters (φ_p, φ_r) can be deduced from the comparison of the results obtained with C_2 and C_3 (Fig. 8.a).

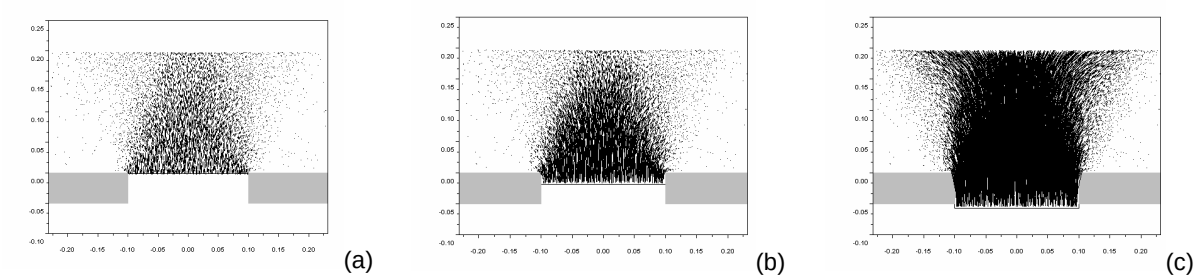

(a) (b) (c)

Figure 7. Displacement field of the particles of the granular layer for material C_1: (a) first phase (δ=6 mm), (b) transitional phase (δ=19 mm), (c) final phase (δ=57 mm).

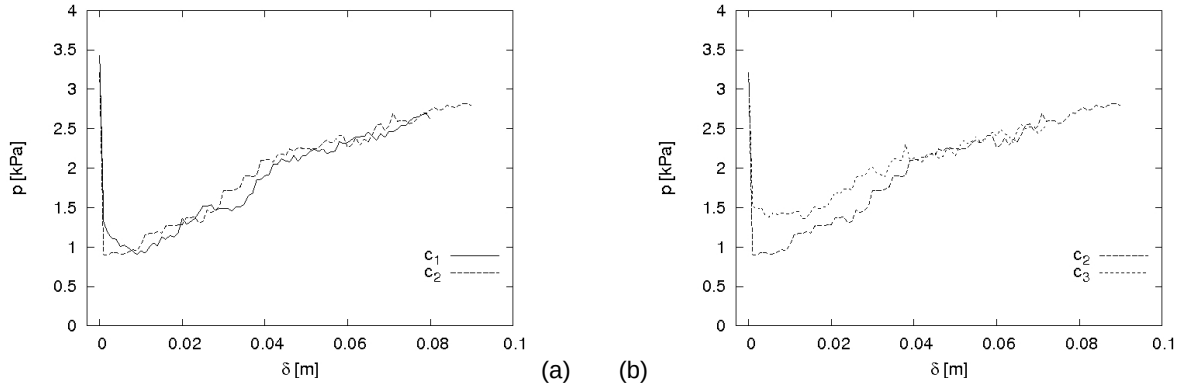

(a) (b)

Figure 8: Numerical results of the trap-door tests p versus δ: (a) C_1 and C_2, (b) C_2 and C_3.

The variations of the pressure acting on the trap-door p with δ are strictly the same for C_1 and C_2 and during the three different phases. No effect of the particle size is recognized in the trap-door problem in the active mode (trap moved downward) as experimentally observed by Tanaka and Sakai (1993).

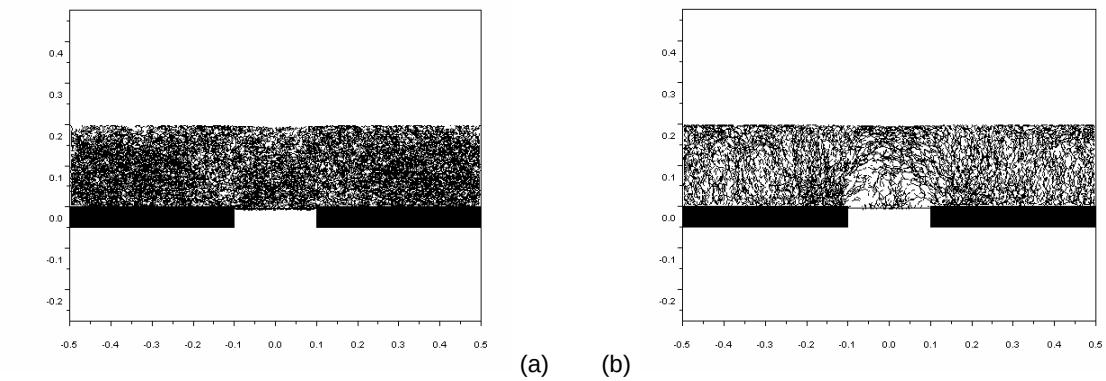

(a) (b)

Figure 9. Contact force distribution in the granular layer: (a) contact forces lower than the mean contact force (in intensity), (b) contact forces higher than the mean contact force (in intensity).

By comparison between results obtained with C_2 and C_3 ($\varphi_p,(C_2)>\varphi_p,(C_3)$ and $\varphi_r(C_2)=\varphi_r(C_3)$), we can deduce from Figure 8.b that the minimal pressure p_{min} observed on the trap-door during the first phase depends on the peak friction angle φ_p as observed in experimental tests with sand and gravel. On the contrary, the final state depends on the critical friction angle φ_r.

Contact forces fields are an accurate way to appreciate how the forces acting in the granular layer are transferred to the stationary part of its support. Two types of forces can be considered: forces with higher intensity than the mean contact force (strong force network) and forces with lower intensity than the mean contact force (weak network). As shown on Fig 9, load transfer pattern is noticeable only within the strong force

network. The weak force network shows a uniform distribution of the weak contact forces in the granular layer.

4 Conclusion

As shown with experimental and numerical results, three phases characterize the trap-door test in the active mode. Each phase corresponds to different load transfer amplitudes. Load transfers amplitude decreases as the displacement of the trap-door increases.
The maximal load transfer phase is observed for very small trap-door displacements. As shown with the numerical model, load transfer amplitude during this phase is related to the peak friction angle.
The classical mechanisms description considering two vertical planes of failure occurs only for largest values of trap-door displacement. The amplitude of load transfers in the final phase is related to the residual friction angle.
The weight of the granular layer is transferred to the stationary parts of the support essentially through the strong contact force network.
The Distinct Element Method allows to reproduce well the trap-door phenomenon and can be applied to determinate the influence of several parameters which are experimentally difficult to control. Influence of size and frictional parameters have been studied, impact of particle shapes and grading need to be investigated.

5 References

Chareyre, B. and Villard, P. 2005. Dynamic Spar Elements and DEM in Two Dimensions for the modelling of soil-Inclusion Problems, *Journal of Engineering Mechanics - ASCE*, **131**(7): 689-698.

Combe G. and Roux J.-N, 2003, Discrete numerical simulation, quasi-static deformation and the origin of strain in granular materials, *3ème Symp. Int. Comportement des sols et des roches tendres*, Eds Di Benedetto et al., pp 1071-1078.

Cundall P.A. and Strack O.D.L., 1979, A discrete numerical model for granular assemblies, *Géotechnique*, **29**, 47-65.

Garca-Rojo R., Hermann H., Mc Namara S. (Eds). 2005. *Powders and Grains 2005: Proceedings of the fifth international conference on the micromechanics of granular media*, Balkema, Rotterdam (The Netherlands).

Handy R. L. 1985. The arch in arching, *Journal of Geotechnical Engineering,* **111**(50), 302-318.

Janssen H.A. 1895. Versuche über Getreidedruck in Silozellen, *Zeitung des Vereins deutscher Ingenieure,* **39**, 1045-1049.

Kolb E., Mazozi T., Clément E., Duran J. 1999. Force Fluctuations in a vertically pushed granular column, *European Physical Journal B,* **8**, 483-491.

Ladanyi B., Hoyaux B. 1969. A study of the trapdoor problem in a granular mass, *Canadian Geotechnical Journal,* **6**(1), 1-15.

Mc Kelvey III J. A. 1994. The anatomy of soil arching, *Geotextiles and Geomembranes,* **13**, 317-329.

Magnier S.A., Donzé F.V., 1994, Spherical Discrete Element Code, in *Element Project Report no. 2*. GEOTOP, Université du Québec à Montréal.

Marston A., Andreson A. O. 1913. The theory of load on pipes ditches and test of cement and clay drain tile and sewer pipes, *Bulletin of the Iowa Engineering Experiment Station*, **31**.

Rankine W. 1857. On the stability of loose earth, *Philosophical Transactions of the Royal Society of London,* **147**.

Rotter J.M., Holst J.M, Ooi J.Y., Sanad A.M. 1998. Silo pressure predictions using discrete-element and finite-element analyses, *Philosophical Transactions of the Royal Society of London A,* **356**, 2685-2712.

Tanaka T., Sakai T. 1993. Progressive failure and scale effect of trap-door problems with granular materials, *Soils and Foundations,* **33**(1), 11-22.

Terzaghi K. 1943. *Theoretical soil mechanics*, J. Wiley & Sons, New York (USA).

Terzaghi K. 1936. Stress distribution in dry and saturated sand above a yielding trap-door, in *Proceedings of International Conference of Soil Mechanics,* Harvard University, Cambridge (USA), **1**, 307-311.

Vanel L., Clément E. 1999. Force Pressure screening and fluctuations at the bottom of a granular column, *European Physical Journal B,* **8**(3), 525-533.

Vardoulakis I., Graf B., Gudehus G. 1981. Trap-door problem with dry sand: a statical approach based upon model test kinematics, *International Journal for Numerical and Analytical Methods in Geomechanics,* **5**, 57-78.

The paper may be considered for
(Please indicate your choice by putting ✓ in the appropriate box)

1. Oral Presentation	✓
2. Poster Session	